LUNAR ROCK DETECTION AND ANALYSIS FOR CHARACTERIZING EROSION PROCESSES. B. Aussel[1] and O. Rüsch[1], [1]Institut für Planetologie, Westfälische Wilhelms-Universität Münster, Germany (aussel.ben@uni-muenster.de, ottaviano.ruesch@uni-muenster.de)

Introduction: To determine the evolution of regolith through erosive processes and for the assessment of possible landing site hazards, information on the distribution and properties of rocks on the lunar surface is crucial [1,2,3]. Currently, high-resolution images of NASA's Lunar Reconnaissance Orbiter (LROC) Narrow Angle Camera (NAC) [4] are the best source available to detect individual boulders. With more than 1.6 million images of which most weren't used in scientific studies yet, an automated detection of lunar boulders would allow a much faster and easier analysis of unmapped regions of interest [e.g. 5].

Methods: Due to the latest improvements in the field of deep learning and computer vision, detecting objects in images can be automated. The goal of our study is to i) automatically detect boulders on the lunar surface and ii) extract physical/geological information based on models [e.g. 1]. We are implementing a Mask R-CNN model based on a preexisting architecture written in Python using the Keras library and a TensorFlow backend [6]. To train the model, we created 256x256 pixel cutouts of calibrated LROC NAC images. The cutouts were visually inspected to access the geologic context and all visible rocks larger than 2 m were mapped with polygons. This process led to much better detections of rocks compared to training with existing rock databases using ellipses. After detection, we model the reflectance profile across the boulder. The expected shape of the reflectance profile is provided by simulated images of boulders based on topographic diffusion modelling (Fig. 4) [1]. With this model, we can get an estimate of the height of the rock and the height of its debris apron (fillet). This reveals information about the surface exposure age and material strength of the boulder [1].

Results: The trained model is able for a given LROC NAC image cutout to detect boulders by delineating a mask around the illuminated part (Fig. 1). These predicted masks usually match well with labelled shape (Fig. 2a). False Positives (FP) can be caused by the rim topography of craters (Fig. 2b) and by small areas of the surface of higher reflectance without topographic relief. Small rocks with a reflectance similar to the background, some of which might represent highly abraded rocks/mounds are the main reason for False Negatives (FN) (Fig. 2c).

The model currently achieves average precisions (AP) between 71 % and 35 % for the detected masks (Fig. 3). These values depend on the Intersection-over-Union (IOU) threshold. The precisions in dependence of the recalls for different IOU thresholds are shown in Fig. 3. As the model is still in development, these results are preliminary.

In a second step, we can extract positions, sizes (length and illuminated area) and shapes for the detected rocks, as well as the reflectance profile in the direction of the sunlight.

As of now, to model the profile, we are combining a so-called "Ricker wavelet" with a gaussian function. In most of the cases, the fitting of the reflectance profile already matches well with the smoothed measured profile (Fig. 5). This demonstrates that in addition to rocks, their debris aprons can be detected and characterized with orbital data in a reproducible way.

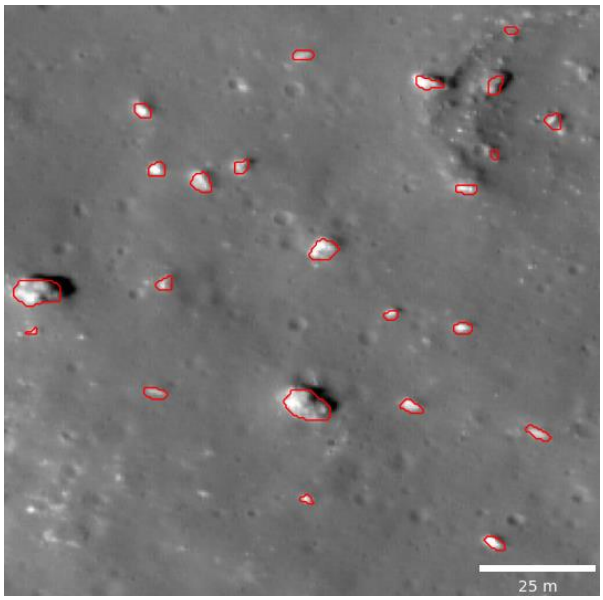

Figure 1*: Example of detections of the model (marked in red) for a subframe of M144931504LE.*

Conclusions: We are developing a Mask R-CNN model that can detect rocks on LROC NAC cutouts. The model can for example be used for the automated creation of size-frequency distribution and thus age maps [7]. As it is still in development further improvements can be achieved. We plan to extend the dataset to get more training data for the model. By using more regions on the Moon, the quality of the data would be improved leading to a better generalization.

The reflectance profiles of the detected rocks can be fitted. The fit can then reveal information about the rock age and strength [1].

References: [1] Rüsch O. and Wöhler C. (2022) *Icarus 384*, 115088, [2] Watkins R. N. et al. (2019) *JGR: Planets 124*, 2754-2771. [3] Li Y. and Wu B. (2018*) JGR: Planets 123*, 1061–1088. [4] Robinson M. S. et al. (2010) *Space Science Review 150*, 81–124. [5] Bickel, V. et al. (2020) *Nature Comm. 11*, 2862. [6] Abdulla W. 'Mask R-CNN' (2017) *Github*. [7] Rüsch, O. et al. (2022) *Icarus 387*, 115200.

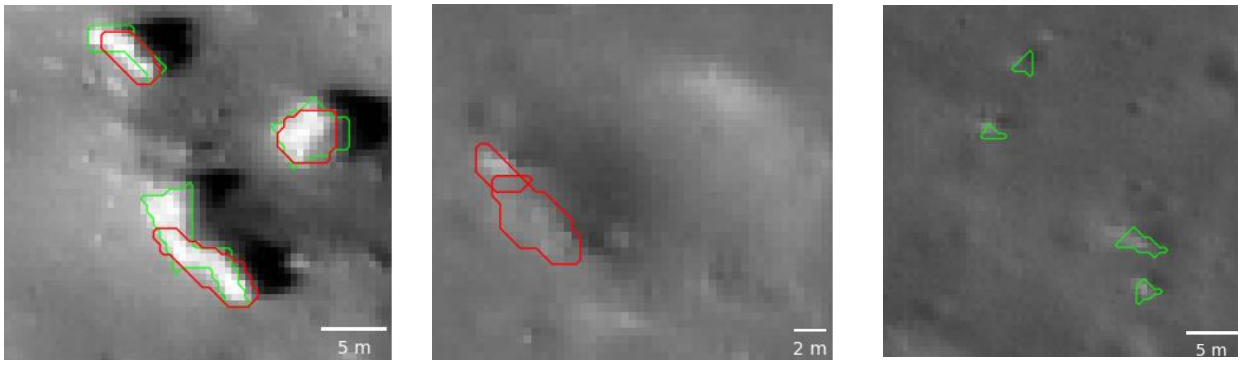

(a) TP (b) FP (c) FN

Figure 2: *Examples of the results (labels marked in green, detections marked in red): (a) True Positives (TP), (b) False Positives (FP) and (c) False Negatives (FN).*

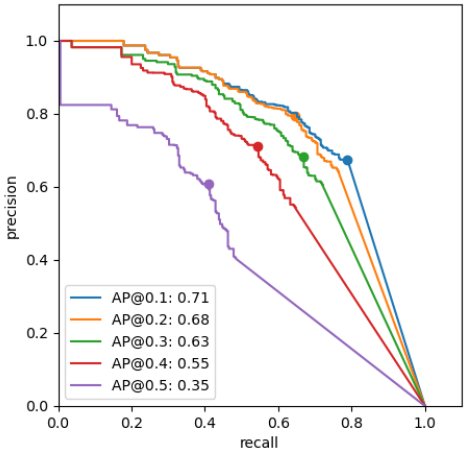

Figure 3: *Precision-recall curve for the model for different IOU thresholds. The marked points state the maximum area under the curve.*

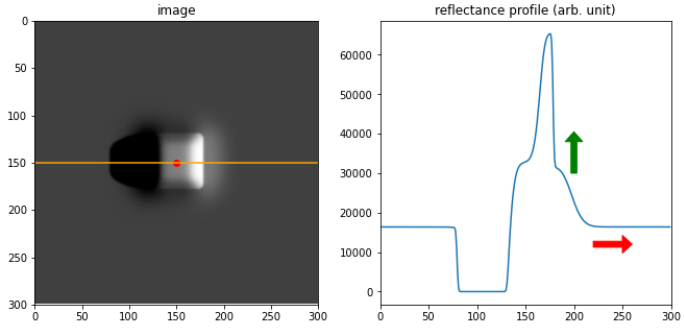

Figure 4: *The maximum reflectance of the fillet is proportional to the rock diffusivity (green arrow) and the width of the fillet is proportional to the rock age (red arrow).*

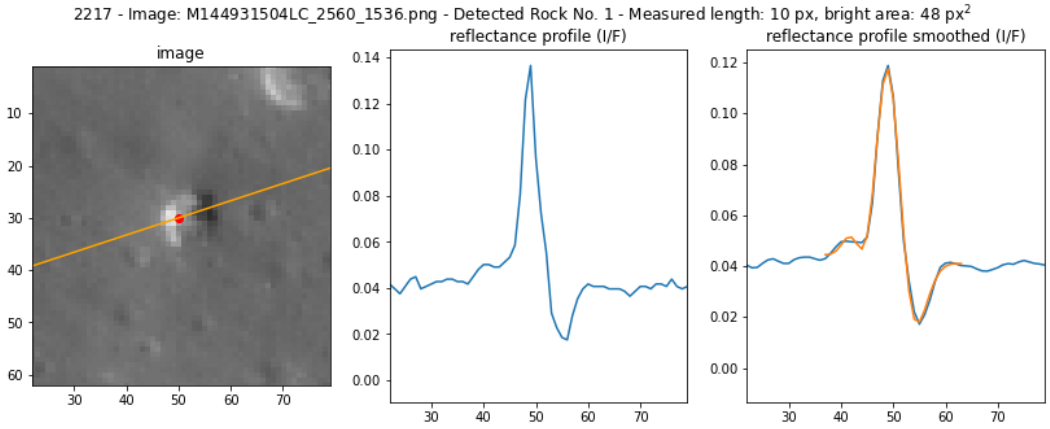

Figure 5: *Example of the analysis of a detected rock. Left: the cutout of the rock with the sunlight direction, middle: the corresponding reflectance profile, right: the smoothed profile (blue) with the calculated fit (orange).*